

MEG: Muon to Electron and Gamma

A. M. Baldini^{1*} and T. Mori²

¹ INFN Pisa, Largo B. Pontecorvo 2, 56127 Pisa, Italy

² ICEPP, The University of Tokyo, 7-3-1 Hongo, Bunkyo-ku, Tokyo 113-0033, Japan

* alessandro.baldini@pi.infn.it

February 11, 2021



Review of Particle Physics at PSI
doi:[10.21468/SciPostPhysProc.2](https://doi.org/10.21468/SciPostPhysProc.2)

Abstract

The possible existence of the $\mu \rightarrow e\gamma$ decay predicted by many new physics scenarios is investigated by stopping positive muons in a very thin target and measuring emitted photons and positrons with the best possible resolutions. Photons are measured by a 2.7 ton ultra pure liquid xenon detector while positron trajectories are measured in a specially designed gradient magnetic field by low-mass drift chambers and precisely timed by scintillation counters. A first phase of the experiment (MEG) ended in 2016, and excluded the existence of the decay with branching ratios larger than 4.2×10^{-13} (90% C.L.). This provides approximately 30 times stronger constraints on a variety of new physics models than previous experiments. In the second phase (MEG II), most of the detectors have been upgraded by adopting up-to-date technologies to improve the search sensitivity by another order of magnitude down to $\mathcal{O}(10^{-14})$. MEG II will pursue new physics beyond the Standard Model complementary to high energy collider experiments with a compatible or even higher sensitivity.

19.1 Introduction: the $\mu \rightarrow e\gamma$ decay

In early 1990's, the precision electroweak measurements at the LEP Collider, CERN, indicated that the electromagnetic, weak, and strong interactions can be unified at $\mathcal{O}(10^{16})$ GeV if TeV-scale supersymmetry exists, hinting strongly at supersymmetric grand unification (SUSY GUT) [1, 2]. It was then shown that sizable lepton flavor violating (LFV) couplings arise naturally in SUSY GUT through the renormalization group evolution, thanks to the heavy top quark, even under the assumption of no flavor mixing at the SUSY breaking scale [3, 4]. Such LFV couplings would lead to an experimentally observable rate of the muon decay, $\mu \rightarrow e\gamma$, which the Standard Model strictly prohibits.

Physicists, fascinated by the possibility of exploring SUSY GUT in muon decays, held a series of workshops in 1997 to design a possible $\mu \rightarrow e\gamma$ search experiment at PSI. PSI was considered to be the best place for such an experiment. This evolved into a Letter of Intent in 1998 [5], which was strongly supported by PSI. A research proposal for a $\mu \rightarrow e\gamma$ experiment [6] was submitted in 1999 and approved by PSI. The experimental collaboration subsequently expanded and named themselves MEG (Mu-E-Gamma) with an updated sensitivity goal of $\mathcal{O}(10^{-13})$ [7].

Discovery of neutrino oscillations in 1998 reinforced the importance of the $\mu \rightarrow e\gamma$ search. Very small neutrino masses implied by the oscillations are naturally explained by the see-saw mechanism. It was shown that the super-heavy right-handed Majorana neutrinos predicted by

41 the see-saw mechanism induce sizable LFV couplings, contributing significantly to the $\mu \rightarrow e\gamma$
42 decay rate in supersymmetric models [8].

43 Lepton flavor conservation is violated in the neutrino oscillations. It is the smallness of
44 the neutrino masses, not lepton flavor conservation, that suppresses the $\mu \rightarrow e\gamma$ decay in the
45 Standard Model extended for finite neutrino masses. Therefore, new physics scenarios that
46 involve heavier particles coupled to leptons, such as supersymmetry or extra dimensions, can
47 naturally produce a measurable rate of the $\mu \rightarrow e\gamma$ decay, making a $\mu \rightarrow e\gamma$ search one of the
48 most powerful tools to access new physics.

49 In the simple 2-body final state of a $\mu \rightarrow e\gamma$ event, an electron and a photon are emitted
50 back-to-back in the rest frame of the decaying muon. Both the electron and the photon have
51 energies equal to half the muon mass (52.8 MeV). To take advantage of this simple 2-body
52 kinematics in the experiment, muons are stopped in a target. Positive muons must be used to
53 avoid formation of muonic atoms, which spoils the 2-body kinematics.

54 The major background in a $\mu \rightarrow e\gamma$ search is the accidental coincidence of a positron from
55 normal muon decay, $\mu \rightarrow e\nu\bar{\nu}$, and a photon from radiative muon decay or the annihilation of
56 a positron in material. The physics background from radiative muon decays, $\mu \rightarrow e\nu\bar{\nu}\gamma$, can
57 be strongly suppressed by good energy and momentum measurements, to levels typically an
58 order of magnitude lower than the accidental background.

59 As the accidental background increases quadratically with the muon rate, a continuous
60 (DC) muon beam rather than a pulsed beam is better suited. To achieve a sensitivity to the
61 branching ratio of $10^{-13} - 10^{-14}$ with a detection efficiency $\epsilon \approx \mathcal{O}(1 - 10 \%)$ in a few years
62 of data taking ($T \approx \mathcal{O}(10^7)$ sec), a DC muon rate of $(10^{13} - 10^{14})/\epsilon/T \approx (10^7 - 10^8)/\text{sec}$ is
63 necessary. Such a high rate DC muon beam is only available at PSI.

64 Both MEG and MEG II experiments were designed to satisfy the following three experi-
65 mental requirements to achieve a sensitivity level of $10^{-13} - 10^{-14}$:

- 66 • *A high intensity DC muon beam of $10^7 - 10^8$ muons/sec.*
- 67 • *A photon detector with excellent energy resolution.* The energy spectrum of the back-
68 ground photons from radiative muon decays and annihilation of positrons in material
69 falls off towards the high energy end of 52.8 MeV. A photon detector with excellent
70 energy resolution can significantly suppress these backgrounds. An innovative liquid
71 xenon scintillation photon detector was developed for MEG. It has a very good intrinsic
72 energy resolution, not limited by impurities, and provides good resolutions in position
73 and timing of photons to discriminate the accidental background.
- 74 • *A precision positron spectrometer that can operate at high rates.* The positron spectrom-
75 eter must be able to make precision measurements in the environment of $10^7 - 10^8$
76 positrons/sec. A positron spectrometer with a gradient magnetic field, called COBRA
77 (COnstant Bending RAdius), was designed together with low mass drift chambers to
78 minimize multiple scattering, and scintillation counters with excellent timing resolution.

79 19.2 The first phase of the experiment: MEG

80 The detector for the first phase of the experiment covered a 10% solid angle, centered around a
81 thin muon stopping target (205 μm -thick polyethylene). The positron spectrometer consisted
82 of a set of drift chambers built at PSI, and scintillation timing counters (TC) located inside a
83 superconducting solenoid with a field varying along the beam axis, from 1.27 T at the center
84 to 0.49 T at each end. The photon detector, located outside the solenoid, was a homogeneous
85 volume (900 l) of liquid xenon (LXe) viewed by 846 UV-sensitive photomultiplier tubes (PMTs)
86 submerged in the liquid. The spectrometer measured the positron momentum vector and
87 timing, while the LXe detector was used to reconstruct the γ -ray energy, as well as the position

88 and time of its first interaction in LXe. All the signals were individually digitized by PSI-
 89 designed waveform digitizers based on the multi-GHz domino ring sampler chip. The π E5
 90 beam line was used to stop 3×10^7 positive muons per second in the target.

91 The MEG detector resolutions and stability were constantly monitored and calibrated. The
 92 LXe detector PMTs were calibrated daily by LEDs and α -sources immersed in the liquid. The
 93 energy scale and resolutions of the LXe detector were measured over the energy range of
 94 4.43 MeV to 129.4 MeV using γ -rays from a radioactive Am/Be source, the (p, γ) -reaction
 95 using a dedicated Cockcroft-Walton accelerator (CW), and $\pi^- p$ charge exchange and radiative
 96 capture reactions. A 9 MeV- γ line from the capture in nickel of neutrons from a pulsed and
 97 triggerable deuteron-deuteron neutron generator allowed the stability of the LXe detector to
 98 be checked even during data-taking. The relative time between the TC and LXe detector was
 99 monitored using radiative muon decay (RMD) and 2γ -events from $^{11}\text{B}(p, 2\gamma)^{12}\text{C}$ reactions.

100 The kinematic variables used to identify the $\mu \rightarrow e\gamma$ decays are the γ -ray and positron
 101 energies (E_γ , E_e), their relative direction ($\Theta_{e\gamma}$) and emission time ($t_{e\gamma}$).

102 The background was largely dominated by the accidental superposition of energetic positrons
 103 from standard Michel muon decay with photons from RMD.

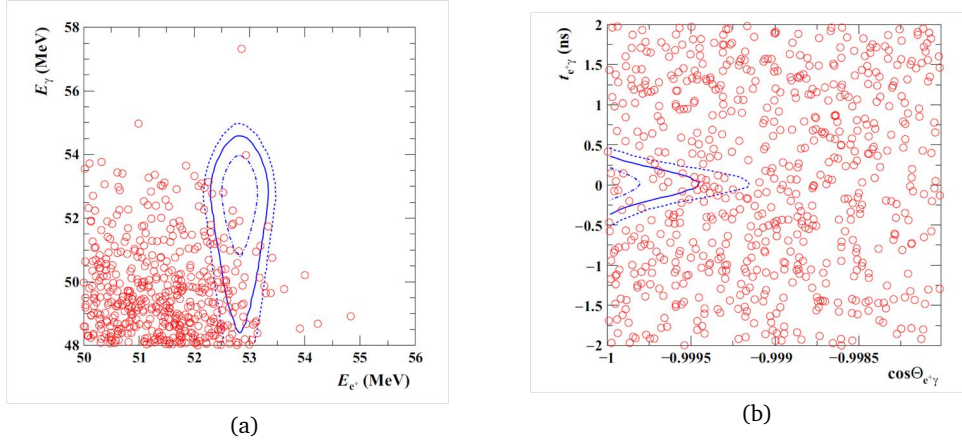


Figure 19.1: MEG final results: (a) E_γ vs E_e (b) $\cos(\Theta_{e\gamma})$ vs $t_{e\gamma}$. 68%, 90% and 95% C.L. signal contour lines are shown.

104 A total of 7.5×10^{14} muons were stopped in the target during the MEG experiment [9].
 105 Figure 19.1 shows the event distributions in the (E_γ, E_e) and $(\cos(\Theta_{e\gamma}), t_{e\gamma})$ planes for the full
 106 data set together with the 68%, 90% and 95% contours of the signal probability distribution
 107 function.

108 A maximum likelihood analysis and a blinding procedure were adopted to examine the
 109 data: events close to the signal region were kept hidden (blind region) until all analysis proce-
 110 dures had been completely defined. The probability density functions needed for the likelihood
 111 analysis were constructed using the events outside of the blind region (sidebands).

112 The analysis shows no evidence for a signal: the final branching ratio upper limit for the
 113 $\mu \rightarrow e\gamma$ decay is 4.2×10^{-13} [9] (90% Confidence Level).

114 While the signal region in Figure 19.1 does not show any significant excess of events, it
 115 does contain background events. This, in short, was the reason for deciding to end MEG data
 116 taking and proceed to a second phase of the experiment with an upgraded detector.

117 The dataset was also used to search for other muon decay modes such as $\mu \rightarrow eX$, $X \rightarrow \gamma\gamma$,
 118 recently suggested by models (see for instance [10]) in which new physics is predicted at low,
 119 rather than high, energy scales. No significant excess was found in the mass range of the axion-
 120 like particle X , $m_X = 20\text{--}45$ MeV/ c^2 and $\tau_X < 40$ ps: the upper limits established [11] were

121 lowered to $O(10^{-11})$ for $m_X = 20\text{--}30 \text{ MeV}/c^2$, up to 60 times more stringent than previous
 122 results [12].

123 19.3 Toward the discovery: MEG II

124 The basic concept of the upgraded MEG experiment – MEG II – is to achieve the highest possible
 125 sensitivity by making full use of the high muon intensity available at PSI: MEG had to reduce
 126 the muon intensity for stable detector operation, and to keep the accidental background at a
 127 sufficiently low level. A significant improvement of the detector resolutions must accompany
 128 the higher muon stopping rate and improved detector efficiency to improve the MEG sensitivity
 129 by an order of magnitude.

130 The main improvements of MEG II over MEG are [13]:

- 131 • *Higher stopping muon rate on target:*
 - 132 – A new single-volume drift chamber with stereo geometry instead of cathode pads
 - 133 for stable long-term operation at the full intensity.
- 134 • *Larger detector acceptance:*
 - 135 – Material mass and distance minimised between the drift chamber and the timing
 - 136 counter, where nearly half of the positrons were lost in the MEG experiment.
 - 137 – Better photon efficiency with lower material mass at the photon entrance face by
 - 138 replacing photomultiplier tubes with silicon photosensors (SiPM).
- 139 • *Improved detector resolutions:*
 - 140 – Better position resolution and more hits per track with the new drift chamber.
 - 141 – A new pixelated timing counter system with straightforward extrapolation of positron
 - 142 trajectory from the drift chamber for improved timing resolution.
 - 143 – Better photon resolutions with more uniform light collection by SiPMs.
 - 144 – A better energy resolution for photons entering near the lateral faces by realigning
 - 145 photomultiplier tubes.
- 146 • *Background suppression:*
 - 147 – A thinner muon stopping target.
 - 148 – A lower-mass drift chamber.
 - 149 – A new device to actively tag the radiative background events.

150 In addition, a unified trigger/digitiser data-acquisition (DAQ) board has been developed
 151 to manage an increased number of read-out channels and a higher bandwidth of the analog
 152 front-end.

153 A sketch of the MEG II experiment is shown in Figure 19.2.

154 Re-tuning the beam line with the full intensity beam to improve the sensitivity, results in
 155 a muon stopping rate of $\sim (5 - 7) \times 10^7 \mu/\text{sec}$. Assuming 120 DAQ days per year, a final
 156 sensitivity of $(5 - 6) \times 10^{-14}$ can be reached in 3-4 years of running, an order of magnitude
 157 better than the final MEG sensitivity. The MEG II proposal was approved by PSI in January,
 158 2013.

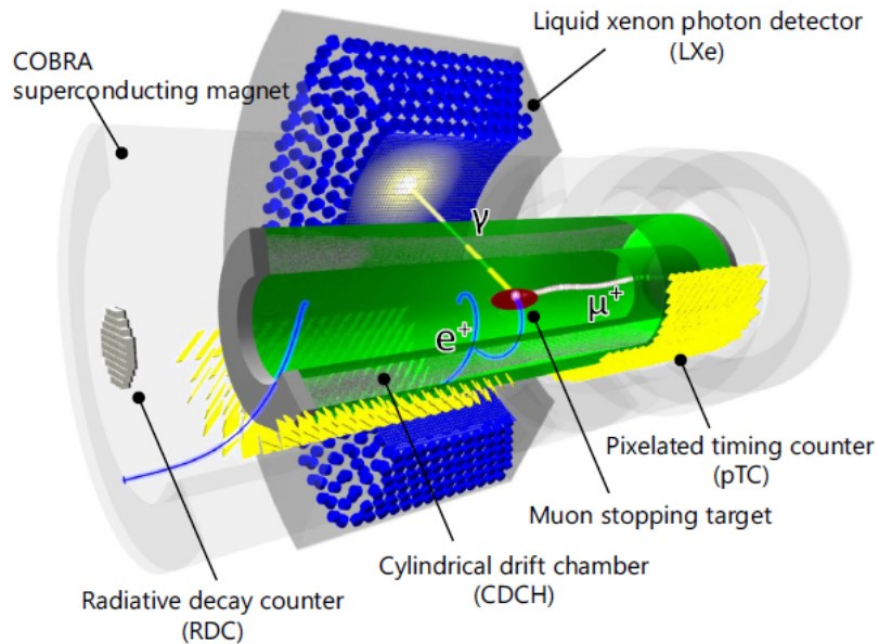


Figure 19.2: A drawing of the MEG II experiment showing its different components

159 19.4 Outlook

160 The MEG II experiment is currently in the detector commissioning phase at the $\pi E5$ beam line.
 161 A small fraction (about 10%) of the read-out electronics channels is available to establish the
 162 optimal data taking conditions. This includes the best beam intensity, the frequency of the
 163 detector maintenance and calibration, the gas mixture for the optimal chamber operation, etc,
 164 so that all the detectors can be operated in their best stable conditions for the entire data-taking
 165 period.

166 After all of the readout electronics is installed in 2021, the experiment will start a full
 167 engineering run. If things go well, physics can then begin. It will be necessary to accumulate
 168 data for three to four years at the $\pi E5$ beam line to achieve the intended sensitivity.

169 Other experiments at PSI, J-PARC in Japan, and FNAL in the U.S., plan to start searches
 170 for other LFV muon processes, $\mu \rightarrow 3e$ [14] (see Section 20 [15]) and $\mu \rightarrow e$ conversion in the
 171 presence of a nucleus [16, 17], in this decade. MEG II, together with these experiments, will
 172 scrutinize an unexplored territory of new physics beyond the Standard Model, which may not
 173 be accessible to the LHC experiments, and could even identify the dynamics of new physics
 174 from a careful comparison of these measurements. It is hoped that MEG II will lead in making
 175 important steps towards our understanding of the fundamental laws of nature.

176 The High Intensity Muon Beam (HIMB) project at PSI [18], aiming at developing new
 177 muon beam lines with intensities up to $10^{10} \mu^+/s$, could have a crucial role in the future for
 178 further studies of $\mu \rightarrow e\gamma$ to clarify new physics. It will require novel experimental technologies
 179 beyond MEG II to keep the backgrounds arising from such high muon intensities under control.

References

- 180
- 181 [1] U. Amaldi, W. de Boer and H. Furstenau, *Comparison of grand unified theories with*
182 *electroweak and strong coupling constants measured at LEP*, Phys. Lett. B **260**, 447 (1991),
183 doi:[10.1016/0370-2693\(91\)91641-8](https://doi.org/10.1016/0370-2693(91)91641-8).
- 184 [2] U. Amaldi, W. de Boer, P. H. Frampton, H. Furstenau and J. T. Liu, *Consistency*
185 *checks of grand unified theories*, Phys. Lett. B **281**, 374 (1992), doi:[10.1016/0370-](https://doi.org/10.1016/0370-2693(92)91158-6)
186 [2693\(92\)91158-6](https://doi.org/10.1016/0370-2693(92)91158-6).
- 187 [3] R. Barbieri and L. Hall, *Signals for supersymmetric unification*, Phys. Lett. B **338**, 212
188 (1994), doi:[10.1016/0370-2693\(94\)91368-4](https://doi.org/10.1016/0370-2693(94)91368-4), [hep-ph/9408406](https://arxiv.org/abs/hep-ph/9408406).
- 189 [4] R. Barbieri, L. J. Hall and A. Strumia, *Violations of lepton flavor and CP in supersymmetric*
190 *unified theories*, Nucl. Phys. B **445**, 219 (1995), doi:[10.1016/0550-3213\(95\)00208-A](https://doi.org/10.1016/0550-3213(95)00208-A),
191 [hep-ph/9501334](https://arxiv.org/abs/hep-ph/9501334).
- 192 [5] A. Van der Schaaf *et al.*, *Letter of Intent to Paul Scherrer Institute, R-98-05.0*, available at
193 <https://meg.web.psi.ch/docs/loi/loi.ps> (1998).
- 194 [6] T. Mori *et al.*, *Research Proposal to Paul Scherrer Institute, R-99-05*, available at
195 https://meg.web.psi.ch/docs/prop_psi/proposal.pdf (1999).
- 196 [7] A. Baldini *et al.*, (*MEG collaboration*). *Research Proposal to INFN*, available at
197 https://meg.web.psi.ch/docs/prop_infn/nproposal.pdf (2002).
- 198 [8] J. Hisano and D. Nomura, *Solar and atmospheric neutrino oscillations and lepton flavor*
199 *violation in supersymmetric models with the right-handed neutrinos*, Phys. Rev. D **59**,
200 116005 (1999), doi:[10.1103/PhysRevD.59.116005](https://doi.org/10.1103/PhysRevD.59.116005), [hep-ph/9810479](https://arxiv.org/abs/hep-ph/9810479).
- 201 [9] A. Baldini *et al.*, *Search for the lepton flavour violating decay $\mu^+ \rightarrow e^+ \gamma$ with the full dataset*
202 *of the MEG experiment*, Eur. Phys. J. C **76**(8), 434 (2016), doi:[10.1140/epjc/s10052-](https://doi.org/10.1140/epjc/s10052-016-4271-x)
203 [016-4271-x](https://doi.org/10.1140/epjc/s10052-016-4271-x), [1605.05081](https://arxiv.org/abs/1605.05081).
- 204 [10] C. Cornella, P. Paradisi and O. Sumensari, *Hunting for ALPs with Lepton Flavor Violation*,
205 JHEP **01**, 158 (2020), doi:[10.1007/JHEP01\(2020\)158](https://doi.org/10.1007/JHEP01(2020)158), [1911.06279](https://arxiv.org/abs/1911.06279).
- 206 [11] A. Baldini *et al.*, *Search for lepton flavour violating muon decay mediated by a new light par-*
207 *ticle in the MEG experiment*, Eur. Phys. J. C **80**(9), 858 (2020), doi:[10.1140/epjc/s10052-](https://doi.org/10.1140/epjc/s10052-020-8364-1)
208 [020-8364-1](https://doi.org/10.1140/epjc/s10052-020-8364-1), [2005.00339](https://arxiv.org/abs/2005.00339).
- 209 [12] R. Bolton *et al.*, *Search for Rare Muon Decays with the Crystal Box Detector*, Phys. Rev. D
210 **38**, 2077 (1988), doi:[10.1103/PhysRevD.38.2077](https://doi.org/10.1103/PhysRevD.38.2077).
- 211 [13] A. Baldini *et al.*, (*MEG collaboration*). *The design of the MEG II experiment*, Eur. Phys. J.
212 C **78**, 380 (2018), doi:[10.1140/epjc/s10052-018-5845-6](https://doi.org/10.1140/epjc/s10052-018-5845-6).
- 213 [14] K. Arndt *et al.*, *Technical design of the phase I Mu3e experiment*, [arxiv:2009.11690v1](https://arxiv.org/abs/2009.11690v1)
214 (2020).
- 215 [15] F. Wauters, *The Mu3e experiment*, SciPost Phys. Proc. **2**, ppp (2021),
216 doi:[10.21468/SciPostPhysProc.2.XXX](https://doi.org/10.21468/SciPostPhysProc.2.XXX).
- 217 [16] R. Abramishvili *et al.*, *COMET Phase-1 Technical Design Report*, Tech. Rep. 2015-1, KEK
218 (2015).

- 219 [17] L. Bartoszek *et al.*, *Mu2e Technical Design Report*, Tech. Rep. 2014-01, Fermilab,
220 doi:[10.2172/1172555](https://doi.org/10.2172/1172555) (2014).
- 221 [18] F. Berg *et al.*, *Target Studies for Surface Muon Production*, *Phys. Rev. Accel. Beams* **19**(2),
222 024701 (2016), doi:[10.1103/PhysRevAccelBeams.19.024701](https://doi.org/10.1103/PhysRevAccelBeams.19.024701), [1511.01288](https://arxiv.org/abs/1511.01288).